The structure of the reaction products of benzene with two and three formal "$BN(i\text{-}Pr)_2$" moieties[2] could be deduced from NMR and mass spectral data. The structure of the product from naphthalene with two formal borene units was finally resolved from spectral data and the hydrolysis products.[1,2] However, NMR spectra of the products of toluene with four added $BN(i\text{-}Pr)_2$ units, **1**, and of *m*-xylene with two additional diisopropylaminoboradiyls, **2**, were too complicated to allow structural assignments. Therefore the structures **1** and **2**, which are obtained according to Scheme I,[6] had to be resolved by X-ray diffraction.[7]

In **1** the aromatic ring is split into C_2 and C_4 units; in **2** the ring has been opened and rearranged with the formation of a cyclopropane ring. In both molecules one C=C double bond is retained. Increased substitution by boron appreciably lengthens the C-C bonds in **1**: C(3a)-C(8a) (1.596 (11)) is substituted by 3B and C(2)-C(5) (1.642 (9) Å) by 4B.

Acknowledgment. Support of this research by Volkswagenstiftung and Fonds der Chemischen Industrie is gratefully acknowledged.

Registry No. 1, 122648-96-8; **2**, 122648-97-9; $F_2BN(i\text{-}Pr)_2$, 38751-90-5; toluene, 108-88-3; *m*-xylene, 108-38-3.

Supplementary Material Available: Listings of crystal data, positional parameters, anisotropic temperature factors, and bond distances and angles for **1** and **2** (11 pages); listings of structure factor amplitudes for **1** and **2** (22 pages). Ordering information is given on any current masthead page.

(6) For the preparation of **1**, 1,3,4,6-tetrakis(diisopropylamino)-8-methyl-1,2,3,3a,4,5,6,8a-octahydro-2,5-cyclo[1,3]diborolo[4,5-*d*]diborepin, and **2**, 3,5-bis(diisopropylamino)-1,8-dimethyl-3,5-diboratricyclo[2.2.2.0^{2,6}]-oct-7-en, respectively, 1.2 mol of Na/K alloy (1:3, 6.9 g of Na + 35.2 g of K) are dispersed in a solution of 2.5 mol of the aromatic compound (230 g of toluene or 260 g of *m*-xylene) and 750 mL of dimethoxyethane (DME). 0.5 mol (74.5 g) of $F_2BN(i\text{-}Pr)_2$ is slowly added with vigorous stirring to this dispersion, and the temperature of the reaction mixture rises to about 35 °C. Stirring is continued for 2 days at room temperature until the alloy solidifies. Then 3.5 g of potassium are added, and stirring is continued 2 more days at reflux temperature. Insoluble materials (alloy and salts) are removed by filtration under N_2 pressure. Solvent and unreacted aromatic compounds are distilled off under reduced pressure. The reaction with toluene delivers 91.5 g of raw products (red oil). High vacuum distillation gives 32.8 g of a yellow oil, bp 90-160 °C/0.01 mbar, which contains mainly $C_7H_8{\cdot}2BN(i\text{-}Pr)_2$ and $C_7H_8{\cdot}3BN(i\text{-}Pr)_2$. Short-path distillation of the residue at 165 °C/0.001 mbar delivers 20.7 g of a highly viscous yellow oil which consists mainly of **1**. The substance shows a tendency to crystallize if it is held at 50 °C. By crystallization from acetone about 10 g of colorless crystals with mp 152 °C are obtained. Anal. Calcd for $C_{31}H_{64}B_4N_4$ (536.13): C, 69.45; H, 12.03; B, 8.07; N, 10.45. Found, MS (FI and EI) 536 (100%): C, 69.52; H, 11.96; B, 8.11; N, 10.41. NMR (only assigned signals are given) $\delta^{11}B$ 46.2 (h/2 840 Hz); δ^1H 1.91 (d, $^4J_{HH}$ 1.1 Hz, CH_3 pos. 8), 5.52 (br, pos. 7); $\delta^{13}C$ 31.78 (CH_3 pos. 8), 128.3 (pos. 8), 162.3 (pos. 7). The reaction with *m*-xylene upon distillation over a 20-cm Vigreux column along with a lower boiling fraction delivers 12.6 g of a colorless oil (bp 101 to 115 °C/0.01 mbar) which solidifies on standing. Recrystallization from acetone gives colorless needles mp 132-133 °C. Anal. Calcd for $C_{20}H_{38}B_2N_2$ (328.15): C, 73.24; H, 12.91; B, 6.59; N, 8.54. Found, MS (FI and EI) 328 (100): C, 73.37; H, 11.62, B, 6.67; N, 8.50. NMR $\delta^{11}B$ 42.6; δ^1H 0.62 (d, $^4J_{H_2/6H_4}$ 1.7 Hz pos. 2/6); 1.36 (s, 3 H, CH_3 pos. 1'), 1.70 (d, 3 H, $J_{Hg'H_7}$ 1.5 Hz, CH_3 pos. 8'), 1.71 (d of t, $^4J_{H_4H_7}$ 1.5 Hz, $^4J_{H_4H_2/6}$ 1.7 Hz pos. 4), 5.27 (d of q, $^4J_{H_7H_8'}$ 1.5 Hz, $^4J_{H_7H_4}$ 1.5 Hz pos. 7); i-Pr (C22) 3.72 (sept), 1.11 + 1.09 (d, $^3J_{HH}$ 6.9 Hz); i-Pr (12) 3.58 (sept), 1.20 + 1.22 (d, $^3J_{HH}$ 6.9 Hz); $\delta^{13}C$ 22.93 (pos. 8'), 25.23 (pos. 1'), 30.89 (br, pos. 2/6), 33.80 (pos. 1), 37.09 (br, pos. 4), 120.72 (pos. 7), 136.17 (pos. 8); i-Pr (C22) 46.81, 24.12, 24.33; i-Pr (C12) 48.43, 23.35, 23.58. Assignments have been made for ^1H by selective decoupling and for ^{13}C by C-H ^1J-correlation and C-H long-range correlation. The numbering (pos.) follows the nomenclature, and in case of the CH_3- and i-Pr groups the numbering correlates with that of Figure 2.

(7) Crystal data for $C_{31}H_{64}B_4N_4$ (**1**) at 20 °C: a = 12.518 (9) Å, b = 19.426 (10) Å, c = 19.357 (10) Å, β = 129.31 (4)°, V = 3642 (6) Å^3, Z = 4, d_{calcd} = 0.98 g cm^{-3}, space group $P2_1/c$. A total of 6360 reflections were measured by using a real-time profile-fitting procedure on a Stoe-Siemens AED. After merging equivalents, 2438 data with $F > 3\sigma(F)$ were used for all calculations (all programs written by author G.M.S.). Final residuals R = 0.114, R_w = 0.081. Crystal data for $C_{20}H_{38}B_2N_2$ (**2**) at 20 °C: a = 6.456 (3) Å, b = 21.850 (17) Å, c = 8.139 (6) Å, β = 112.57 (5)°, V = 1060 (2) Å^3, Z = 2, d_{calcd} = 1.03 g cm^{-3}, space group $P2_1/m$. 3936 data were measured, after merging 1161 with $F > 3\sigma(F)$ used for all calculations. Final residuals R = 0.060, R_w = 0.057. A riding model with idealized hydrogen geometry was employed for H-atom refinement in both structures.

Resonance Raman Spectrum of the Lowest Triplet State of Zinc(II) Tetraphenylporphyrin

Valerie A. Walters,[1a] Julio C. de Paula,[1b]
Gerald T. Babcock,* and George E. Leroi*

Department of Chemistry and the LASER Laboratory
Michigan State University
East Lansing, Michigan 48824-1322

Received June 13, 1989

Porphyrin-based macrocycles in low-energy excited electronic states are involved in a number of important biological processes, including excitation energy transfer and charge separation. To gain insight into the detailed mechanisms by which the excited macrocycles perform their functions, knowledge of the conformation and electronic structure of the participating electronic state is needed. Previous resonance Raman investigations of metalloporphyrin excited states have focused on d,d states.[2] Here, we report the time-resolved resonance Raman (TR^3) spectrum of the lowest π,π^* triplet state of Zn(II) tetraphenylporphyrin (ZnTPP). The number of observed vibrational bands is consistent with a lowering of the point group symmetry of the porphyrin core (excluding phenyl rings) from the D_{4h} symmetry of the ground electronic state, which we attribute to the Jahn-Teller effect previously predicted for the T_1 state.[3] In addition, the electronic excitation appears to be localized on the porphyrin ring alone and does not extend to the phenyl rings.

Figure 1 shows the TR^3 spectrum (1150-1650 cm^{-1}) from T_1 of ZnTPP in tetrahydrofuran (Figure 1a) and methylcyclohexane (Figure 1b).[4] The T_1 state was populated with a ~10-ns pulse of 532-nm radiation and probed with a second ~10-ns pulse with a wavelength (460 nm) chosen to coincide with the maximum of the triplet-triplet absorption curve.[5] Bands are observed at the same frequencies in the two solvents. From the absence of observable scattering at 1551 cm^{-1}, where the ground state (S_0) exhibits a strong band (Figure 1c), we conclude that all the labeled peaks in the TR^3 spectra are attributable to scattering from the T_1 state of ZnTPP.

Consistent with this assignment are the kinetics of the recovery of the ground-state spectrum. With increasing time delay between laser pulses, the intensities of the T_1 bands decrease and those of the S_0 bands increase, yielding a time constant of several hundred microseconds. This decay time is shorter than the triplet lifetime obtained optically,[6] owing to triplet-triplet annihilation processes[5b,7] that occur for the more concentrated samples required for the resonance Raman experiment.

Analysis of the TR^3 spectrum yields information on the structure of the porphyrin in the triplet excited state. The two

(1) (a) Current address: Department of Chemistry, Lafayette College, Easton, PA 18042. (b) Current address: Department of Chemistry, Haverford College, Haverford, PA 19041.

(2) (a) Findsen, E. W.; Shelnutt, J. A.; Ondrias, M. R. *J. Phys. Chem.* **1988**, *92*, 307-314. (b) Apanasevich, P. A.; Kvach, V. V.; Orlovich, V. A. *J. Raman Spectrosc.* **1989**, *20*, 125-133. (c) Chikishev, A. Y.; Kamalov, V. F.; Koroteev, N. I.; Kvach, V. V.; Shkurinov, A. P.; Toleutaev, B. N. *Chem. Phys. Lett.* **1988**, *144*, 90-95.

(3) Gouterman, M. *Ann. N.Y. Acad. Sci.* **1973**, *206*, 70-83.

(4) The pump pulse was the second harmonic from a Quanta-Ray Nd:YAG laser. The probe pulse was obtained from a Quanta-Ray dye laser pumped by a second Nd:YAG laser. The time delay between pulses was controlled by a Stanford Research Corp. digital delay generator, which triggered both lasers. Photons scattered from the excited state were collected in a SPEX Triplemate monochromator and detected with a PAR 1420 intensified diode array detector. A low-temperature (-80 °C) backscattering apparatus was used to obtain the T_1 spectra. The spectral resolution was approximately 8 cm^{-1}. Samples were degassed to prevent quenching of the triplet state. The integrity of all samples was monitored by UV-vis spectra obtained before and after irradiation, which establish that none of the peaks in Figure 1 are due to decomposition products.

(5) (a) Rodriguez, J.; Kirmaier, C.; Holten, D. Accepted for publication in *J. Am. Chem. Soc.* (b) Pekkarinen, L.; Linschitz, H. *J. Am. Chem. Soc.* **1960**, *82*, 2407-2411.

(6) Triplet lifetime is 1.2 ms at 300 K and 26 ms at 77 K in methylcyclohexane, as reported in the following: Darwent, J.; Douglas, P.; Harriman, A.; Porter, G.; Richoux, M.-C. *Coord. Chem. Rev.* **1982**, *44*, 83-126.

(7) Harriman, A. *J. Chem. Soc., Faraday Trans. 2* **1981**, *77*, 1281-1291.

0002-7863/89/1511-8300$01.50/0

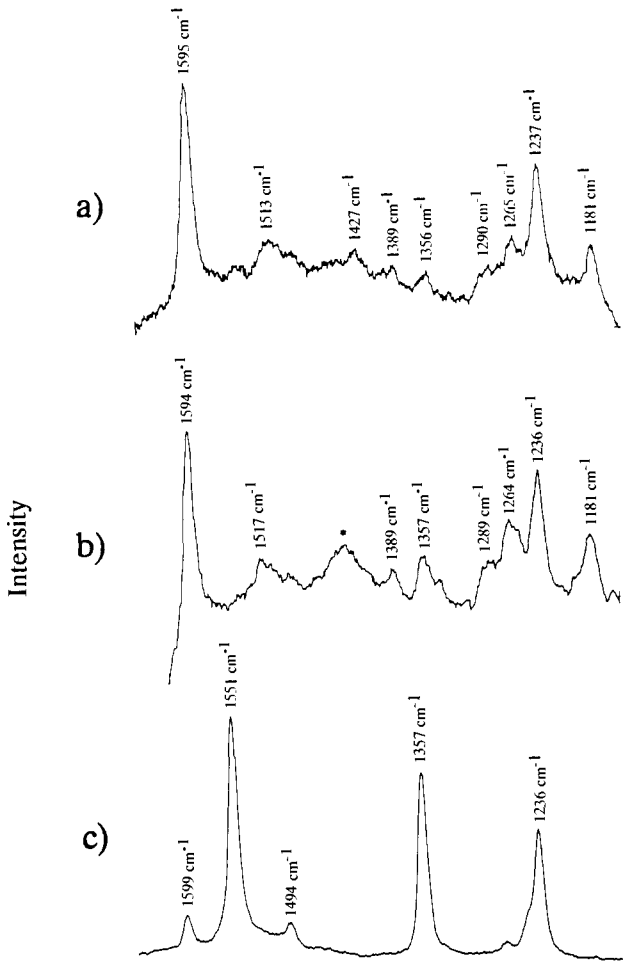

Figure 1. Time-resolved resonance Raman spectrum of the lowest triplet state of ZnTPP in (a) tetrahydrofuran and (b) methylcyclohexanne. For the spectrum in THF (Alfa, ultrapure 99%), 100 mW of the pump pulse (532 nm) and 40 mW of the probe pulse (460 nm) were used. The delay between the pump and probe beams was 50 ns. No solvent scattering was observed due to the high ZnTPP concentration (1×10^{-3} M.) For b, the 50-mW probe beam was delayed from the 200-mW pump beam by 100 ns. Scattering from the methylcyclohexane solvent (Aldrich, 99% spectrophotometric grade) obtained under similar power and temperature conditions has been subtracted. Sample concentration was ca. 3×10^{-4} M. (The starred peak at ca. 1440 cm^{-1} is due to incompletely subtracted solvent contributions.) Trace c shows the resonance Raman spectrum of the ground electronic state of ZnTPP in CS_2 (Fisher Scientific, spectranalyzed) obtained with 45 mW of 457.9-nm radiation from a Spectra-Physics Model 165 Ar ion laser. The signal was obtained from the room-temperature solution (not degassed) in a 90° scattering configuration. Other conditions are as in footnote 4. The S_0 frequencies were not observed to be solvent dependent; similar frequencies were observed by using methylcyclohexane or THF as solvent.

strongest T_1 bands, at 1594 and 1236 cm^{-1} (in Figure 1b), are assigned to phenyl vibrations on the basis of the following considerations. Bands at similar wavenumbers appear in the ground-state spectra of ZnTPP and related metal-substituted tetraphenylporphyrins,[8] where they are assigned to the $C_{ph}C_{ph}$ stretch and the C_mC_{ph} inter-ring stretch, respectively. The corresponding modes in the ground state of ZnTPP-d_{20} (in which the phenyls are deuterated) are at 1564 cm^{-1} and 1185 cm^{-1}, respectively, and we observe strong bands at these frequencies in the T_1 Raman spectrum of ZnTPP-d_{20} (data not shown). The observation of similar frequencies and isotope shifts for these modes in the T_1 and S_0 states suggests that the potential-energy distributions and assignments for the phenyl modes are similar in the ground and excited states (see Table I). Moreover, the 1594-cm^{-1} and 1236-cm^{-1} modes in S_0 have a_{1g} symmetry, and the corresponding excited-state bands are found to be polarized. The lack of frequency shift between the ground and triplet excited states leads us to conclude that no substantial geometry change (with accompanying electronic redistribution) occurs in the phenyl modes as a result of the excitation to the T_1 state. We conclude that the electronic changes are localized to the porphyrin ring alone and that phenyl–porphyrin conjugation in the T_1 state does not occur.

Table I. Vibrational Band Assignments for the T_1 State of ZnTPP

mode	frequencies, cm^{-1} T_1	S_0	character[b]	symmetry
ϕ_4	1594 (1564)[a]	1599 (1564)[a]	$C_{ph}C_{ph}$	a_{1g}
ν_2	1517, 1495[c]	1551	C_aC_m, C_bC_b	a_{1g}
ν_{10}		1585[b]	C_aC_m	b_{1g}
ν_{11}	1427	1494	C_bC_b	b_{1g}
ν_4	1389	1357	C_aC_b, C_aN	a_{1g}
ν_{27}	1264	1269[b]	C_mC_{ph}	b_{2g}
ν_1	1236 (1186)[a]	1236 (1185)[a]	C_mC_{ph}	a_{1g}
ϕ_6	1181	1181[b]	$C_{ph}C_{ph}H$	a_{1g}

[a] Frequencies in parentheses are for the corresponding band in ZnTPP-d_{20}. [b] From ref 8a,b. [c] Our data do not allow us to distinguish between ν_2 and ν_{10} in T_1.

The lack of frequency shift in the T_1 phenyl modes implies that the use of the porphyrin localized orbitals of Gouterman's four-orbital model is appropriate in the T_1 state. This is consistent with the resonance Raman spectra for the TPP anion[8a,9] and cation radicals.[10] Neither addition of an electron to the e_g orbital (anion) nor removal of an electron from the a_{2u} orbital (cation) has any effect on the frequency of the phenyl ring modes. Hence, it is not surprising that promotion of an electron from the a_{2u} orbital to the e_g orbital to form the T_1 state also does not cause a shift in the frequencies of the phenyl modes. The large scattering cross section of the phenyl modes in T_1 most likely reflects delocalization of electrons onto the phenyl rings in the higher energy triplet state (T_n) in resonance with the 460-nm probe beam.

The lowest triplet state of ZnTPP has E_u symmetry and purportedly results from an $a_{2u}e_g$ configuration, which is not mixed with the near-degenerate triplet state having $a_{1u}e_g$ configuration.[11] This is in contrast to the case for the two lowest excited singlet states, for which strong configuration interaction results in nearly equal mixtures of the two configurations. Configuration interaction acts to minimize the Jahn–Teller effect normally expected for doubly degenerate states.[12] In the triplet states, where configuration interaction is not symmetry allowed,[11b] Jahn–Teller effects should be manifest.[3] Indeed, EPR experiments yield a nonzero value for the zero field splitting parameter, E, providing strong evidence that the lowest triplet state of ZnTPP is Jahn–Teller distorted.[13] Jahn–Teller distortion in D_{4h} molecules can occur along b_{1g} and/or b_{2g} normal coordinates, causing b_{1g} and b_{2g} vibrational modes, respectively, to become totally symmetric in the reduced symmetry. Such modes can have nonzero intensity in resonance Raman spectra via Franck–Condon scattering. This is analogous to the case of the ZnTPP anion radical[8a] (E_g ground state), where additional bands were assigned to b_{1g} modes. In the TR[3] spectra there appear to be more bands in the 1650–

(8) (a) CuTPP and ZnTPP$^-$: Atamian, M.; Donohoe, R. J.; Lindsey, J. S.; Bocian, D. F. *J. Phys. Chem.* **1989**, *93*, 2236–2243. (b) NiTPP: Li, X.-Y.; Czernuszewicz, R. S.; Spiro, T. G. *J. Phys. Chem.* In press. The mode labels used in the text are those of ref 8b.

(9) Yamaguchi, H.; Soeta, A.; Toeda, H.; Itoh, K. *J. Electroanal. Chem. Interfacial Electrochem.* **1983**, *159*, 347–359.
(10) Czernuszewicz, R. S.; Macor, K. A.; Li, X.-Y.; Kincaid, J. R.; Spiro, T. G. *J. Am. Chem. Soc.* **1989**, *111*, 3860–3869.
(11) (a) Gouterman, M. *J. Chem. Phys.* **1960**, *33*, 1523–1529. (b) Ake, R. L.; Gouterman, M. *Theor. Chim. Acta* **1969**, *15*, 20–42. (c) Gouterman, M.; Howell, D. B. *J. Chem. Phys.* **1974**, *61*, 3491–3492. (d) Petke, J. D.; Maggiora, G. M.; Shipman, L. L.; Christofferson, R. E. *J. Mol. Spectrosc.* **1978**, *71*, 64–84.
(12) (a) Cheung, L. D.; Yu, N.-T.; Felton, R. H. *Chem. Phys. Lett.* **1978**, *55*, 527–530. (b) Shelnutt, J. A.; Cheung, L. D.; Chang, R. C. C.; Yu, N.-T.; Felton, R. H. *J. Chem. Phys.* **1977**, *66*, 3387–3398.
(13) (a) Langhoff, S. R.; Davidson, E. R.; Gouterman, M.; Leenstra, W. R.; Kwiram, A. L. *J. Chem. Phys.* **1975**, *62*, 169–176. (b) van der Waals, J. H.; van Dorp, W. G.; Schaafsma, T. J. In *The Porphyrins*; Dolphin, D., Ed.; Academic Press: New York, 1978; Vol. 4, pp 257–312.

1150-cm^{-1} region than in the ground-state spectrum. We attribute these additional bands to symmetry lowering resulting from Jahn–Teller distortion, and these bands can be correlated to non totally symmetric modes (b_{1g} or b_{2g}) in the ground state.

Assignments for most of the vibrational bands in the T_1 state are found in Table I. We have already assigned the 1594-cm^{-1} mode to the $C_{ph}C_{ph}$ stretch (ϕ_4) and the 1236-cm^{-1} band to the C_mC_{ph} stretch (ν_1). If we assume that all phenyl modes in the T_1 state are unshifted, we can assign the 1181-cm^{-1} band to a $C_{ph}C_{ph}H$ bend (ϕ_6), in accord with the calculated ground-state assignment.[8] Likewise, the T_1 1264-cm^{-1} band is correlated to the 1269-cm^{-1} band (ν_{27}) of b_{2g} symmetry in the S_0 state (of NiTPP and CuTPP) which has C_mC_{ph} character. Consideration of the porphyrin molecular orbital diagrams[14] permits prediction of the direction of frequency shifts for the porphyrin skeletal modes[15] upon excitation to the T_1 state; the porphyrin modes involving predominantly C_aC_m or C_bC_b stretching motions should decrease, and modes primarily associated with C_aC_b or C_aN stretches should increase in frequency. In Table I, the T_1 1517-, 1495-, 1427-, and 1389-cm^{-1} bands are assigned to porphyrin modes. The T_1 1357- and 1289 cm^{-1} bands are probably due to b_{1g} or b_{2g} modes (D_{4h} symmetry designations) which become active through the Jahn–Teller effect.

Acknowledgment. We are grateful to Prof. D. Holten and Dr. C. Kirmaier for valuable discussions and advice. We also thank Dr. M. Atamian for helpful discussions on the normal coordinate analysis of TPPs and Dr. A. Salehi and Prof. C. K. Chang for providing the ZnTPP-d_0 and ZnTPP-d_{20}. J.C.dP. thanks the NIH for a postdoctoral fellowship (Grant No. GM12383). This work was also funded in part by NIH Grant GM25480 (G.T.B.) and NSF Grant CHE87-22111 (G.E.L.).

(14) Gouterman, M. *J. Mol. Spectrosc.* **1961**, *6*, 138–163. Predictions were made by using the a_{2u} molecular orbital coefficients of Maggiori: Maggiori, G. M. *J. Am. Chem. Soc.* **1973**, *95*, 6555–6559.

(15) A similar approach was successfully applied in the case of metalloporphyrin cation radicals. See, for example: Oertling, W. A.; Salehi, A.; Chang, C. K.; Babcock, G. T. *J. Phys. Chem.* **1989**, *93*, 1311–1319. See also ref 10.

A Novel Ribose C-4′ Hydroxylation Pathway in Neocarzinostatin-Mediated Degradation of Oligonucleotides

Isao Saito,* Hiroshi Kawabata, Tsuyoshi Fujiwara, Hiroshi Sugiyama, and Teruo Matsuura

Department of Synthetic Chemistry
Faculty of Engineering, Kyoto University
Kyoto 606, Japan
Received April 3, 1989

Currently, there is considerable interest in the mechanism of sequence-selective DNA damage by the action of antitumor antibiotic neocarzinostatin (NCS).[1] Upon incubation with thiol, NCS chromophore generates a highly reactive species, plausibly a biradical species derived from an NCS chromophore thiol adduct,[2] which abstracts a hydrogen normally from C-5′ of DNA deoxyribose.[1,3] Recent demonstration that synthetic hexanucleotides can act as a sequence-selective substrate for NCS[4] or NCS chromophore[5] has provided a particularly useful tool for establishing the chemical structure of the DNA lesion induced by NCS and clarifying the mechanism leading to its formation. Here we report that previously unobserved C-4′ hydroxylation of deoxyribose occurs significantly at T_3 in competition with normal C-5′ hydrogen abstraction from deoxyribose at A_4 in NCS-mediated degradation of self-complementary hexanucleotide d(CGTACG).[5,6]

Scheme I

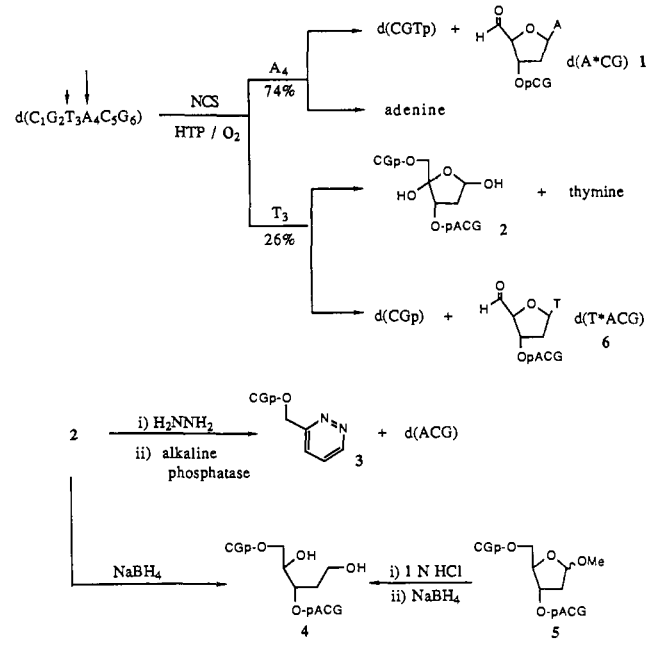

A typical reaction mixture (50 μL) containing NCS (250 μM), d(CGTACG) (42 μM strand concentration), and 4-hydroxythiophenol (HTP, 4 mM)[4] as an NCS activator in 50 mM Tris·HCl buffer (pH 7.2) was incubated at 0 °C for 12 h under aerobic conditions.[7] When the reaction mixture was treated with hot alkali (0.5 M NaOH, 90 °C, 5 min), formation of free thymine and adenine was detected by reverse-phase HPLC in a ratio of ca. 1:3, suggesting that NCS attacks T_3 and A_4 sites in a similar ratio.[5] Direct analysis of the reaction mixture by reverse-phase HPLC[8] indicated the formation of three major products, d(CGTp), 5′-aldehyde fragment d(A*CG) (**1**), and unknown product, together with several minor products including free adenine and thymine as indicated in Scheme I. The structure of **1** was established by quantitative reduction to d(ACG) by $NaBH_4$ (0.05 M, 0 °C, 15 min). Collection of the HPLC peak of the unknown product followed by enzymatic digestion with snake venom phosphodiesterase and alkaline phosphatase gave dG, dC, and dA in a ratio of 2:2:1. Treatment of the fraction[9] with aqueous hydrazine (0.1 M, 90 °C, 5 min) followed by alkaline phosphatase digestion cleanly produced pyridazine derivative **3**[10] and d(ACG). The structure of **3** was confirmed by comparison of its HPLC

(1) Goldberg, I. H. *Free Radical Biol. Med.* **1987**, *3*, 41 and references therein.

(2) (a) Myers, A. P.; Proteau, P. J.; Handel, T. M. *J. Am. Chem. Soc.* **1988**, *110*, 7212. (b) Myers, A. G.; Proteau, P. J. *Ibid.* **1989**, *111*, 1146.

(3) (a) Kappen, L. S.; Goldberg, I. H. *Biochemistry* **1983**, *22*, 4872. (b) Kappen, L. S.; Goldberg, I. H. *Nucleic Acids Res.* **1985**, *13*, 1637 and references therein.

(4) (a) Kawabata, H.; Sugiyama, H.; Tashiro, T.; Takeshita, H.; Matsuura, T.; Saito, I.; Ito, A.; Koide, Y. *Nucleic Acids Symp. Ser.* **1988**, *No. 20*, 69. (b) Kawabata, H.; Takeshita, T.; Fujiwara, H.; Sugiyama, H.; Matsuura, T.; Saito, I. *Tetrahedron Lett.* **1989**, *30*, 4263.

(5) Lee, S. H.; Goldberg, I. H. *Biochemistry* **1989**, *28*, 1019.

(6) Hydrogen abstraction at C-1′ of deoxyribose giving 2-deoxyribonolactone has recently been reported at the d(AGC) sequences in NCS chromophore mediated degradation of oligonucleotides: Kappen, L. S.; Goldberg, I. H. *Biochemistry* **1989**, *28*, 1027.

(7) In a control experiment in the absence of HTP or NCS, oxidation of the hexamer never proceeded even after 24-h incubation under the conditions. The disappearance rate of d(CGTACG) in the presence of NCS was ca. 50% of that observed for d(GCATGC)[4] upon incubation with HTP under identical conditions. HTP- and 2-mercaptoethanol-activated NCS showed exactly the same sequence selectivity in cleaving 5′-end labeled 261-bp DNA fragments.

(8) HPLC conditions: Wakosil 5C_{18} ODS column; 0.05 M triethylammonium acetate containing 3–14% acetonitrile, linear gradient, 20 min; flow rate 1.5 mL/min; retention time (d(CGTp)) 10 min, (**1**) 12 min, (**2**) 14.5 min.

(9) Evaporation of the fraction to dryness under reduced pressure below 10 °C resulted in a rapid decomposition of **2** to d(CGp), d(CG), d(pACG), and d(ACG) as revealed by HPLC.

(10) Sugiyama, H.; Xu, C.; Murugesan, N.; Hecht, S. M.; van del Marel, G. A.; van Boom, J. H. *Biochemistry* **1988**, *27*, 58.

0002-7863/89/1511-8302$01.50/0